NeuroImage: Clinical 18 (2018) 793–801

Contents lists available at ScienceDirect

NeuroImage: Clinical

journal homepage: www.elsevier.com/locate/ynicl

Dynamic network dysfunction in cocaine dependence: Graph theoretical metrics and stop signal reaction time

Yihe Zhang[a,b], Sheng Zhang[b], Jaime S. Ide[b], Sien Hu[b,c], Simon Zhornitsky[b], Wuyi Wang[b], Guozhao Dong[a], Xiaoying Tang[a,*], Chiang-shan R. Li[b,d,e,f,**]

[a] Department of Biomedical engineering, School of Life Sciences, Beijing Institute of technology, Beijing, China
[b] Department of Psychiatry, Yale University School of Medicine, New Haven, CT, USA
[c] Department of Psychology, State University of New York, Oswego, NY, USA
[d] Department of Neuroscience, Yale University School of Medicine, New Haven, CT, USA
[e] Interdepartmental Neuroscience Program, Yale University School of Medicine, New Haven, CT, USA
[f] Beijing Huilongguan Hospital, Beijing, China

ARTICLE INFO

Keywords:
Substance use disorders
Cocaine
Connectivity
Graph metrics
Response inhibition
Inhibitory control

ABSTRACT

Graphic theoretical metrics have become increasingly popular in characterizing functional connectivity of neural networks and how network connectivity is compromised in neuropsychiatric illnesses. Here, we add to this literature by describing dynamic network connectivities of 78 cocaine dependent (CD) and 85 non-drug using healthy control (HC) participants who underwent fMRI during performance of a stop signal task (SST). Compared to HC, CD showed prolonged stop signal reaction time (SSRT), consistent with deficits in response inhibition. In graph theoretical analysis of dynamic functional connectivity, we examined temporal flexibility and spatiotemporal diversity of 14 networks covering the whole brain. Temporal flexibility quantifies how frequently a brain region interacts with regions of other communities across time, with high temporal flexibility indicating that a region interacts predominantly with regions outside its own community. Spatiotemporal diversity quantifies how uniformly a brain region interacts with regions in other communities over time, with high spatiotemporal diversity indicating that the interactions are more evenly distributed across communities. Compared to HC, CD exhibited decreased temporal flexibility and increased spatiotemporal diversity in the great majority of neural networks. The graph metric measures of the default mode network negatively correlated with SSRT in CD but not HC. The findings are consistent with diminished temporal flexibility and a compensatory increase in spatiotemporal diversity, in association with impairment of a critical executive function, in cocaine addiction. More broadly, the findings suggest that graph theoretical metrics provide new insights for connectivity analyses to elucidate network dysfunction that may elude conventional measures.

1. Introduction

Neural phenotypes serve as diagnostic or prognostic marker of neuropsychiatric illnesses and numerous studies have shown altered brain activity or connectivity in individuals with cocaine addiction. For instance, dependent cocaine users demonstrated diminished resting state functional connectivity (rsFC) of the salience network, seeded from the insula, as compared to non-drug using controls (Geng et al., 2017). In a treatment cohort, rsFC between right temporal pole and medial prefrontal cortex (MPFC) predicted relapse status at 150 days. Another study demonstrated disrupted interactions between default mode and salience networks in cocaine addiction (Liang et al., 2015). RsFC decreased between the orbitofrontal/dorsal PFC and ventral striatum and increased between dorsal and ventral striatum in abstinent cocaine users, particularly in those who relapsed to drug use (Berlingeri et al., 2017). RsFC among executive and salience networks were higher among individuals who remained abstinent after treatment (McHugh et al., 2017). Spectral dynamic causal modeling showed altered effective connectivity of the mesolimbic circuit involving the ventral tegmental area, nucleus accumbens and MPFC in cocaine users (Ray et al., 2016). In our recent study with multivariable pattern analysis, rsFC of thalamic subregions distinguished cocaine users from non-drug using controls at a higher accuracy, in comparison with brain regions with similar volumes (Zhang et al., 2016).

* Correspondence to: X. Tang, 715-3 Teaching Building No. 5, Beijing Institute of technology, 5 South Zhongguancun Road, Beijing 100081, China.
** Correspondence to: C.-S. R. Li, Connecticut Mental Health Center S112, 34 Park Street, New Haven CT 06519-1109, USA.
E-mail addresses: xiaoying@bit.edu.cn (X. Tang), chiang-shan.li@yale.edu (C.-s.R. Li).

https://doi.org/10.1016/j.nicl.2018.03.016
Received 2 November 2017; Received in revised form 9 January 2018; Accepted 14 March 2018
Available online 16 March 2018

Other studies addressed task-related functional connectivity. In a finger tapping task requiring variable speed response, MPFC connectivity with the basal ganglia was decreased in cocaine users, particularly at higher speed, compared to controls (Lench et al., 2017). Compared to non-drug using controls, abstinent cocaine users showed increased left dorsolateral prefrontal cortical (DLPFC) connectivity with the putamen in response to increasing reward magnitude in a counting Stroop task blocked with varying monetary rewards (Rosell-Negre et al., 2016). Current cocaine users demonstrated reduced amygdala connectivity with the anterior cingulate cortex (ACC) in response to angry and fearful facial expressions, compared to controls (Crunelle et al., 2015). In another study cocaine addicted individuals relative to non-drug using pathological gamblers exhibited enhanced connectivity between the ventral caudate and subgenual ACC, in link with steeper delay discounting and relapse to drug use (Contreras-Rodriguez et al., 2015). Dynamic causal modeling showed altered prefrontal striatal connectivity during response inhibition in a go/nogo task in cocaine users (Ma et al., 2015). Combining fMRI of cue-induced craving and a Bayesian search algorithm to identify the causal circuits of craving, investigators reported a positive correlation between the strength of the causal influence of the insula on the DLPFC and craving rating (Ray et al., 2015b).

Together, these and many other studies highlighted changes in functional connectivity during resting or task challenges in cocaine misuse (Adinoff et al., 2015; Albein-Urios et al., 2014; Barros-Loscertales et al., 2011; Caldwell et al., 2015; Cisler et al., 2013; Hu et al., 2015c; Konova et al., 2015; Ma et al., 2014; McHugh et al., 2014; Ray et al., 2015a; Wisner et al., 2013; Zhang et al., 2014). The great majority of these studies focused on specific regions of interest, and none examined the dynamic aspects of functional connectivity (Cohen, 2017).

The bulk of connectivity studies assume that functional connectivity over the data collection period (or chronnectome) is relatively static (Calhoun et al., 2014). This assumption was challenged in studies of time-varying connectivities (Sakoğlu et al., 2010). A rationale is that because of physiological noise, scanner drift, and fluctuation of participants' attention, functional connectivity may not be truly static (Morgan et al., 2015). As also shown in task-based fMRI, brain regions showed a trend toward decreasing activation as participants continued to perform on the same task (Menon and Uddin, 2010). These considerations prompted studies to capitalize on the wealth of information contained within the temporal features of BOLD signals (Hutchison et al., 2013).

More importantly, the coordination of brain activity between neural populations is a dynamic and context-dependent process. Brain dynamics give rise to variations in complex network properties over time, possibly achieving a balance between efficient information processing and metabolic expenditure (Zalesky et al., 2014) and potentially playing a critical role in supporting cognition (Allen et al., 2014; Calhoun et al., 2014; Chang and Glover, 2010; Kang et al., 2011; Thompson et al., 2013). Given sufficient data, a number of metrics could be used to characterize dynamic connectivity (Hutchison et al., 2013). For instance, in a study of network connectivity of the insula using a “sliding window” approach, dynamic states mirrored the cognition-emotion-interoception divisions observed of static networks, with both overlapping and unique connectivity profiles (Nomi et al., 2016). The results highlight how dynamic connectivity better characterizes functional connections of insula subdivisions and suggest more nuanced models of insula function. A study of temporal lobe epilepsy reported that as seizures progress over the years, dynamic connectivity measures showed declining functional independence of the ipsilateral from the midline cingulate network (Morgan et al., 2015). Thus, dynamic connectivity quantifies widespread network alterations and their evolution over the duration of the disease, providing a severity or treatment outcome marker of epilepsy. Together, these and other studies (Damaraju et al., 2014; de Lacy et al., 2017; Kaiser et al., 2016; Sakoğlu et al., 2010; Yaesoubi et al., 2017) highlight the utility of dynamic functional connectivity (DFC) in capturing the neural processes that may be critical to the etiology of neuropsychiatric conditions.

Here we investigated how whole-brain DFC may be altered in cocaine addicted individuals in contrast to non-drug using controls. Specifically, we employed graph theoretical analyses with temporal flexibility and spatiotemporal diversity as two indices to examine how networks of brain regions interact over time (Alnaes et al., 2015; Bassett et al., 2011; Chen et al., 2016; Fornito et al., 2012). Temporal flexibility characterizes how frequently a brain region interacts with regions outside its own community across time. Spatiotemporal diversity reflects how uniformly a brain region interacts with regions in other communities over time.

With a within-subject design, we compared these graph theoretical metrics of imaging data collected during the stop signal task (SST) between cocaine users and controls. On the basis of previous work (Cai et al., 2017; Cai et al., 2016; Cai et al., 2014; Duann et al., 2009; Hu et al., 2016; Zhang and Li, 2010, 2012), we hypothesized that the medial frontal, frontoparietal task control and salience networks as well as the default mode network (DMN) demonstrate altered graph metrics in cocaine dependent individuals, in association with impaired response inhibition, as compared to non-drug using controls.

2. Materials and methods

2.1. Subjects and behavioral task

Eighty-five healthy control (HC) and 78 cocaine dependent (CD) adults participated in this study. CD resided in an inpatient treatment unit and was abstinent between 1 and 2 weeks before fMRI scan was conducted. All participants reported no major medical, neurological, or other psychiatric illnesses (except nicotine use disorder), denied use of other illicit substances and tested negative for cannabis, opioids, amphetamine, methamphetamine, phencyclidine, benzodiazepine, and barbiturate on the day of fMRI. All participants signed a written, informed consent in accordance with a protocol approved by the Yale Human Investigation Committee.

Participants performed a stop signal task or SST, which was described in details in our previous studies (Bednarski et al., 2012; Hu et al., 2014; Winkler et al., 2013; Zhang et al., 2014). Briefly, a “go” signal set up a pre-potent response tendency in go trials (~75%), and an additional, less frequent “stop” signal instructed subjects to withhold their response in stop trials (~25%). Go and stop trials were randomized in presentation, with an inter-trial-interval of 2 s. The time delay between go and stop signal – stop signal delay (SSD) – was staircased, increasing and decreasing by 67 ms each following a stop success and error trial. Participants were instructed to respond as quickly as they could to “go” signal, while watching out for the “stop” signal. In the scanner, participants completed four 10-minute runs of the SST, with approximately 100 trials in each run. With the staircase procedure, participants succeeded in stopping approximately half of time. The stop signal reaction time (SSRT) – the time needed for one to stop the response half of the time, was estimated on the basis of a race model. Briefly, in the race model, go and stop processes independently race toward a finish line and whichever finishes first determines the trial outcome. With the race model, the SSRT can be estimated by subtracting a critical SSD (where subjects would succeed in stopping half of the time) from the mean go trial RT. The SSRT indexes the capacity of response inhibition, with shorter SSRT reflecting better ability of inhibitory control.

2.2. Imaging protocol

Conventional T1-weighted spin-echo sagittal anatomical images were acquired for slice localization using a 3-T scanner (Siemens Trio,

Erlangen, Germany). Anatomical images of the functional slice locations were obtained with spin-echo imaging in the axial plane parallel to the anterior commissure–posterior commissure (AC–PC) line with TR = 300 ms, TE = 2.5 ms, bandwidth = 300 Hz/pixel, flip angle = 60°, field of view = 220 × 220 mm, matrix = 256 × 256, 32 slices with slice thickness = 4 mm and no gap. A single high-resolution T1-weighted gradient-echo scan was obtained. One hundred seventy-six slices parallel to the AC–PC line covering the whole brain were acquired with TR = 2530 ms, TE = 3.66 ms, bandwidth = 181 Hz/pixel, flip angle = 7°, field of view = 256 × 256 mm, matrix = 256 × 256, 1 mm^3 isotropic voxels. Functional scans were conducted with the SST. Blood oxygenation level dependent (BOLD) signals were acquired with a single-shot gradient-echo echo-planar imaging (EPI) sequence. Thirty-two axial slices parallel to the AC–PC line covering the whole brain were acquired with TR = 2000 ms, TE = 25 ms, bandwidth = 2004 Hz/pixel, flip angle = 85°, field of view = 220 × 220 mm, matrix = 64 × 64, 32 slices with slice thickness = 4 mm and no gap. There were 10 min (three hundred images) in each run for a total of four runs of the SST.

2.3. Data pre-processing

All data were first analyzed with Statistical Parametric Mapping (SPM, Wellcome Department of Imaging Neuroscience, University College London, U.K.). In the pre-processing of BOLD data, images of each participant were realigned (motion-corrected) and corrected for slice timing. A mean functional image volume was constructed for each participant for each run from the realigned image volumes. These mean images were co-registered with the high resolution structural image and then segmented for normalization to a Montreal Neurological Institute EPI template with affine registration followed by nonlinear transformation (Ashburner and Friston, 1999; Friston et al., 1995). Images were then smoothed with a Gaussian kernel of 8 mm at full width at half maximum. A multiple linear regression with 12 realignment parameters (3 translations, 3 rotations, and their first temporal derivatives) was applied to the smoothed data. Averaged signals from predefined white matter and cerebrospinal fluid masks were computed, detrended, and regressed out of the preprocessed data. The first 5 frames of BOLD data were discarded to enable the signal to achieve steady-state equilibrium between radio frequency pulsing and relaxation. Finally, for each subject, data were concatenated across the four runs of SST for analyses.

2.4. Graph model metrics

We largely followed (Chen et al., 2016) in the computation of graph metrics. The workflow is summarized in Fig. 1.

2.4.1. Node definition

Nodes were defined from Power's atlas with 264 brain regions. The 264 nodes were grouped to form 14 large scale networks, including the salience network (SN), cingulo-opercular task control network (CON), fronto-parietal task control network (FPN), dorsal attention network (DAN), ventral attention network (VAN), subcortical network, default mode network (DMN), memory retrieval network, visual network, auditory network, sensory-motor networks as well as the cerebellum network (Power et al., 2011; Power et al., 2013). Voxel signals were extracted, detrended and averaged for each node. A band-pass filter (0.008 Hz < f < 0.25 Hz) was applied to remove low-frequency signal drifts and increase the signal noise ratio.

2.4.2. Time varying functional connectivity

A sliding window with no gap or overlap between windows was applied to the time series to obtain dynamic functional connectivity between nodes. Exponentially decaying weights were applied to each time point within a window (Zalesky et al., 2014). The exponentially decaying weights were computed as:

$$w_t = w_0 e^{(t-T)/\theta},\ t = 1,\ ..., T$$

where $w_0 = (1 - e^{-1/\theta})/(1 - e^{-T/\theta})$, t is the t^{th} time point within the sliding window, T is the window length (= 40 s), and the exponent θ controls the influence from distant time points, set to a third of the window length. Connectivity matrix for each time window was obtained by computing the weighted Pearson correlation between the time-series of any two nodes x_t and y_t as:

$$r_w = \frac{\sum_{t=1}^{T} w_t (x_t - \bar{x})(y_t - \bar{y})}{\sqrt{\sum_{t=1}^{T} w_t (x_t - \bar{x})^2} \sqrt{\sum_{t=1}^{T} w_t (y_t - \bar{y})^2}}$$

where $\bar{x} = \frac{\sum_{t=1}^{T} w_t x_t}{T}$ and $\bar{y} = \frac{\sum_{t=1}^{T} w_t y_t}{T}$. The resulting connectivity matrix for each window was z-transformed within the subject for subsequent analysis.

2.4.3. Modularity

Modularity was used to determine the optimal community structure within the unthresholded connectivity matrix by grouping nodes into non-overlapping communities or modules that maximize intra-modular connectivity and minimize inter-modular connectivity (Newman, 2004). Louvain community detection algorithm from the Brain Connectivity Toolbox (Rubinov and Sporns, 2010) was employed to identify community structure in both static and time-varying connectivity matrices. The algorithm optimizes a quality function Q, defined as the difference between the observed intra-modular and inter-modular connectivity, while penalizing assignment of nodes with negative correlations to the same community. The algorithm was repeated 100 times and the results with the highest Q was extracted as the optimal community structure, for the computation of group static matrix and each subject's temporal co-occurrence matrix.

2.4.4. Temporal co-occurrence matrix

To investigate dynamic interactions between nodes, temporal co-occurrence matrices were computed based on subject's optimal community structures as obtained from the time-varying connectivity matrix. The community structure within each sliding window was used to construct an adjacency matrix A_{ijtk}, such that $A_{ijtk} = 1$ if node i and node j are in the same community within time window t for participant$k$, otherwise $A_{ijtk} = 0$. The temporal co-occurrence matrix was thus computed as the temporal mean of the adjacency matrix $C_{ijk} = \frac{\sum_{t=1}^{T} A_{ijtk}}{T}$ (Bassett et al., 2015; Braun et al., 2015; Mattar et al., 2015). Each element measures the proportion of times that two nodes are part of the same community. A higher value indicates that the two corresponding nodes participate in the same community more frequently.

2.4.5. Group static functional connectivity

Two levels of static functional connectivity were defined and computed. At the first level, for each individual, the static connectivity between nodes was computed by applying Pearson correlations on the nodes' time-series. At the second level, the resulting correlation matrices from individual subjects were z-transformed and averaged to form a group averaged connectivity matrix. Modularity analysis was performed with random initialization for 100 times on group averaged connectivity matrix to determine the optimal static community structure, to be used for the computation of node-level metrics.

2.4.6. Node-level metrics

With the temporal co-occurrence matrix C_{ijk} and the group static community, we characterized the dynamic spatiotemporal properties of each node using two measures: temporal flexibility and spatiotemporal diversity.

The temporal flexibility of node i and participant k was computed as:

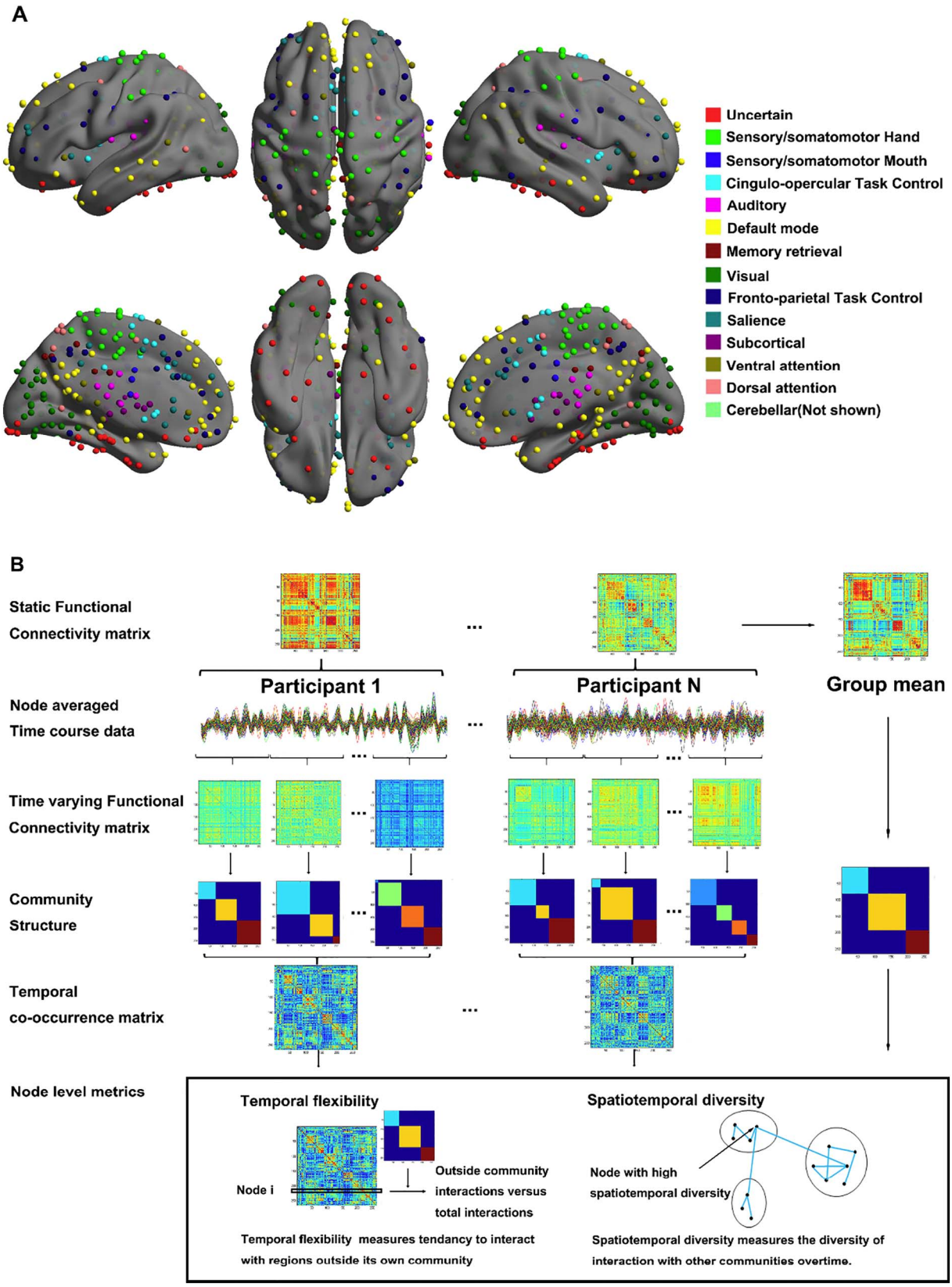

Fig. 1. Analysis workflow. (**A**) 264 regions (nodes) representing the entire brain and encompassing key (static) large-scale brain networks, including the SN, CON, FPN, DAN, VAN, subcortical, DMN, memory systems, visual, auditory, sensory-motor, and the cerebellum. (**B**) Time-varying changes in the community structure of intrinsic functional connectivity were quantified using a sliding window approach. An optimized community detection algorithm was used to compute a temporal co-occurrence matrix and graph metrics – temporal flexibility and spatiotemporal diversity – to characterize dynamic functional interactions between brain regions.

$$f_{ik} = \frac{\sum_{j \notin u_i} C_{ijk}}{\sum_{j \neq i} C_{ijk}}$$

where C_{ijk} is the temporal co-occurrence matrix for individual k, u_i is the community to which node i belongs, and $\Sigma_{j \notin u_i} C_{ijk}$ measures the total frequency with which node i interacts with nodes outside its native community (Mucha et al., 2010). Temporal flexibility of the node captures the tendency of deviation from its own native community and interaction with nodes from other community.

The spatiotemporal diversity of node i and participant k was computed as:

$$h_{ik} = -\frac{1}{\log(m)} \sum_{u \in M} p_{ik}(u) \log p_{ik}(u)$$

where $p_{ik}(u) = \frac{s_{ik}(u)}{s_{ik}}$, s_{ik} is the degree/strength of node i among all communities for participant k, $s_{ik}(u)$ is the degree/strength of node i in community u for participant k, m is the total number of communities, and M is the set of communities (Fornito et al., 2012). Nodes with high spatiotemporal diversity scores are those that have relatively spatially varied distribution of time-varying interactions with all communities and are putative loci for integrating information between communities.

2.4.7. Correlation with behavioral performance

We used both Pearson correlation to examine the relationship between graph metrics and the stop signal reaction time (SSRT), the primary outcome measure of the SST. We focused on four networks that are known to be associated with inhibitory control – the saliency network, default mode network (DMN), cingulo-opercular network (CON), and fronto-parietal network (FPN) – in Pearson regression with the two connectivity metrics – temporal flexibility and spatiotemporal diversity. A corrected p value of 0.05/8 = 0.0063 was used to examine the correlation results.

3. Results

3.1. Dynamic functional interactions

For both CD and HC, we used the temporal co-occurrence matrix to compute dynamic functional connectivity (temporal flexibility and spatiotemporal diversity) in association with each brain node, with the findings grouped according to the 14 networks (Fig. 2). Temporal flexibility is a measure of how frequently a brain region interacts with regions belonging to other communities across time. High temporal flexibility indicates that a region predominantly interacts with regions outside its own community. Spatiotemporal diversity is a measure of how uniformly a brain region interacts with regions in other communities over time. High spatiotemporal diversity indicates that interactions are more evenly distributed across communities. Crucially, brain regions with high temporal flexibility may not have high spatiotemporal diversity if they predominantly interact with brain regions in only one community; therefore, spatiotemporal diversity provides complementary information about the spatial distribution of time-varying connectivity. Because a total of 14 networks were tested, we employed a corrected p value of 0.05/14 = 0.0036 to evaluate the results of independent sample t-tests. The results showed that temporal flexibility was significantly decreased for all except auditory ($p = 0.1136$) and subcortical ($p = 0.0164$) networks in CD, as compared to HC. In contrast, spatiotemporal diversity was significantly increased for all except sensory motor hand ($p = 0.9614$) and frontopaietal ($p = 0.0485$) networks in CD as compared to HC.

To examine whether CD and HC differed in these neural metrics as a result of disparity in SSRT, we conducted an analysis of variance (ANOVA) with group (CD vs. HC) and SSRT (short vs. long; median split in each group) on temporal flexibility and spatiotemporal diversity of each network. At the corrected threshold ($p = 0.0036$), all except the subcortical and auditory networks showed a significant group main effect in temporal flexibility (p's $< 3.97e-08$). The DMN was the only network showing a significant SSRT main effect ($p = 0.0008$). There were not significant group by SSRT interaction effects in temporal flexibility. For spatiotemporal diversity, all except the saliency, frontoparietal task control, and somatomotor mouth networks showed a significant group main effect (p's < 0.0009). There was not significant SSRT main effect or group by SSRT interaction effects. The statistics were shown in the Supplement.

3.2. Dynamic parameters of the default mode network (DMN) are correlated with SSRT

We compared SST outcome measures of CD and HC. The result showed that, compared to HC, CD was prolonged in SSRT (236 ± 53 vs. 225 ± 44 ms; $t = 2.0334$, $p < 0.05$; independent sample t-test).

We performed pairwise Pearson regression on SSRT and each of the eight network connectivity metrics (four networks × two metrics) and examined the results with a corrected $p = 0.0063$, each for CD and HC. In CD the temporal flexibility of the DMN negatively correlated with SSRT ($r = -0.4492$; $p < 0.000037$). Also in CD the spatiotemporal diversity was negatively correlated with SSRT ($r = -0.3338$; $p < 0.0029$). Fig. 3 shows scatter plots of the DMN graph measures in linear regression with SSRT. No other correlations were significant under the corrected threshold (Table 1). Notably, the Pearson r values were negative for all correlations, indicating that greater temporal flexibility and spatiotemporal diversity of these networks are associated with shorter SSRT or better inhibitory control. Without considering correction for multiple comparisons, the temporal flexibility of the DMN and salience network was negatively correlated with SSRT in HC, and the spatiotemporal diversity of the frontoparietal network and salience network was negatively correlated with SSRT in HC and CD, respectively (all p's < 0.05).

4. Discussion

4.1. Network dysconnectivity in cocaine addiction

Temporal flexibility of the default-mode network (DMN) decreased in cocaine dependent (CD) as compared to healthy control (HC) participants. Compared to HC, CD showed prolonged stop signal reaction time (SSRT), reflecting an impairment in the capacity of response inhibition. Temporal flexibility of the DMN correlated negatively with the SSRT in CD and, less significantly, in HC. Thus, higher temporal flexibility of the DMN is associated with better inhibitory control across CD participants. This finding suggests that a greater extent at which the DMN interacts with nodes from other communities is associated with expedient response inhibition, particularly for CD. These findings are broadly consistent with earlier reports of disrupted DMN activity and connectivity in association with altered self-referential functions, emotion and memory, and coordination between internal and external stimuli in cocaine addiction (Bednarski et al., 2011; Geng et al., 2017; Konova et al., 2015; Liang et al., 2015; Matuskey et al., 2013).

To consider whether the two graph metrics varied between CD and HC independent of task performance, we conducted a group by SSRT ANOVA. The results confirmed that temporal flexibility and spatiotemporal diversity of the great majority of networks remained significantly different and that there were no significant interaction effects. The results suggest that these connectivity measures are altered in cocaine addiction independent of task performance. On the other hand, as expected, the DMN showed a significant SSRT main effect in temporal flexibility. The latter finding along with a lack of interaction effect suggests that one cannot rule out the possibility that differences in DMN connectivity to some extent reflect disparity in the capacity of inhibitory control.

Compared to HC, CD showed increased spatiotemporal diversity of the DMN. Further, spatiotemporal diversity of the DMN was negatively

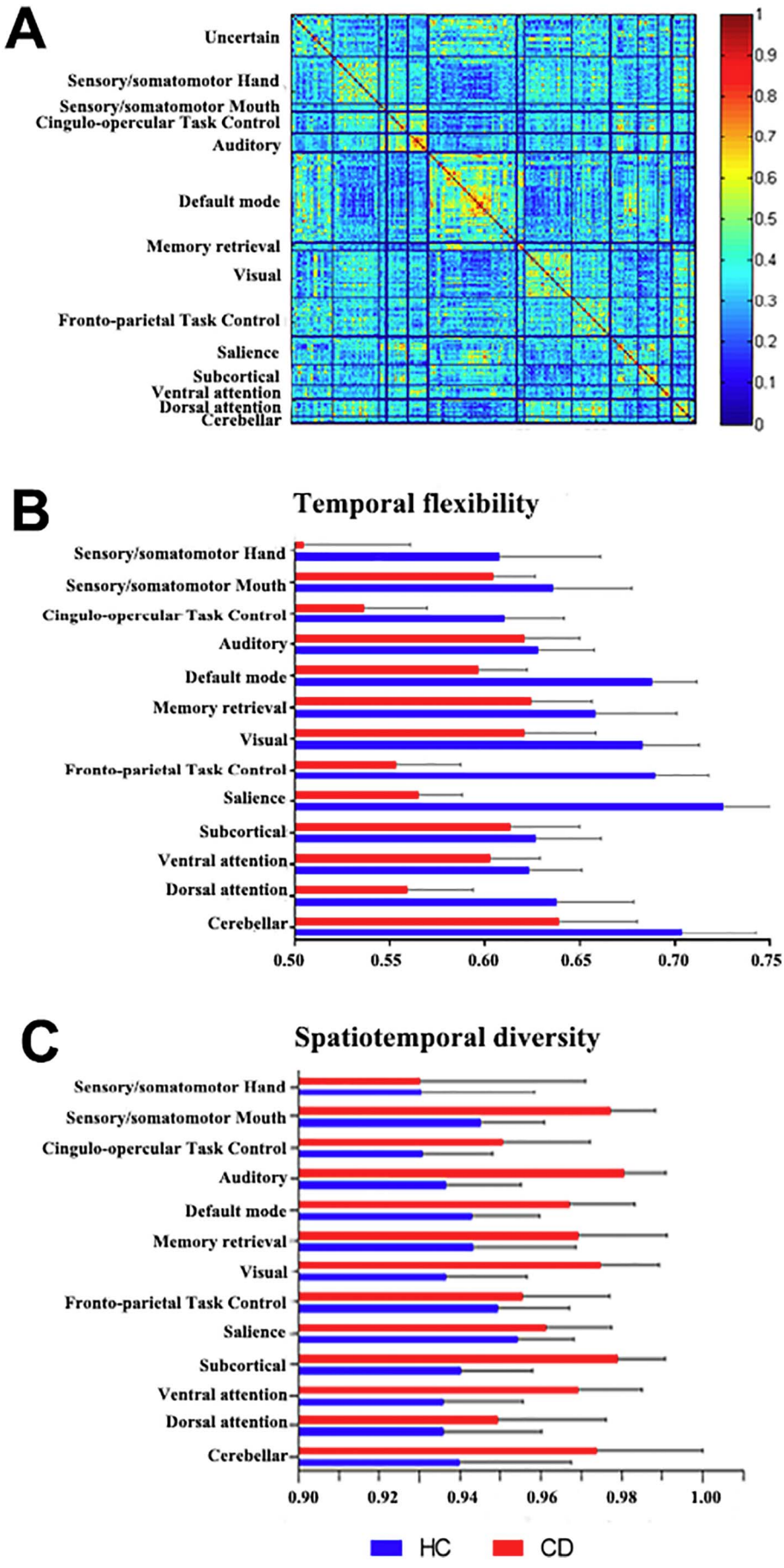

(caption on next page)

Fig. 2. Temporal co-occurrence matrix and time-varying graph model metrics of CD and HC. (**A**) Temporal co-occurrence matrix for the 264 brain nodes ordered and labeled according to the 14 networks. (**B**) Temporal flexibility, averaged across nodes, of each network. (**C**) Spatiotemporal diversity, averaged across nodes, of each network. All data bars show mean ± standard deviation.

correlated with SSRT in CD but not HC. Broadly in accord with earlier work demonstrating both decreased and increased functional connectivity (Ray et al., 2015a), this finding likely reflects a compensatory process in CD. As spatiotemporal diversity measures how uniformly a brain region interacts with regions in other communities over time, with higher spatiotemporal diversity indicating more evenly distributed interactions across communities, CD may compensate by recruiting interactions across multiple networks to support stop signal performance (Barros-Loscertales et al., 2011; Ide et al., 2016; Ide et al., 2015; Li et al., 2008; Zhang et al., 2014; Zhang et al., 2016). These networks likely cover an extensive array of brain regions to support all of the individual component processes of cognitive control, such as attention, response inhibition, error monitoring and post-error behavioral adjustment. Along with temporal flexibility, spatiotemporal diversity captures the network dynamics critical to response inhibition and how the network functions may be disrupted in cocaine addicted individuals.

Table 1
Correlation between network graph measures and SSRT.

			DMN	SN	CON	FPN
Temporal flexibility vs. SSRT	HC	r	−0.27603	−0.25036	−0.19099	−0.19621
		p	**0.01056**	**0.02083**	0.07995	0.07190
	CD	r	−0.44916	−0.18400	−0.15531	−0.18429
		p	**3.71e-5***	0.10683	0.17453	0.10628
Spatiotemporal diversity vs. SSRT	HC	r	−0.20607	−0.20384	−0.19115	−0.22420
		p	0.05847	0.06131	0.07971	**0.03914**
	CD	r	−0.33376	−0.26794	−0.18621	−0.20924
		p	**0.00282***	**0.01771**	0.10261	0.06598

Note: p values < 0.05 are in bold. DMN: default mode network; SN: saliency network; CON: cingulo-opercular network; FPN; frontoparietal network.
* Significant at a corrected $p < 0.0063$.

4.2. Dynamic connectivity metrics as an additional etiological feature

As described earlier, in addition to the DMN, brain regions of the saliency, fronto-parietal and cingulo-opercular networks have shown activity and connectivity responses in relation to executive control dysfunction in cocaine addiction. In contrast to the largely localized findings, the current results of graph metrics of dynamic connectivity highlight a distinct role of the DMN in relation to response inhibition impairment. The capacity of response inhibition, as indexed by the stop signal reaction time (SSRT), has conventionally be conceptualized as a reactive control process – the SSRT quantifies the time needed to interrupt the motor response as instructed by the stop signal. However, more recent studies have described an elaborate neural network, including the DMN, for proactive control and how proactive control interacts with reactive processes to support response inhibition (Hu et al., 2015a; Hu et al., 2015b; Ide et al., 2013). In addition, earlier studies showed that fluctuation in activity of the perigenual anterior cingulate cortex (pgACC), an important node of the DMN, may reflect moment-to-moment changes in attention and is critically linked to stop signal performance, with higher pgACC activities predicting an impending stop error (Bednarski et al., 2011; Li et al., 2007). These additional dimensions of cognition understandably have not been routinely considered in work of response inhibition. Along with these earlier studies, the current findings highlight the complexity of cognitive processes and the utility of dynamic connectivity measures in capturing some of these interactive processes that may conduce to inhibition function and dysfunction.

Similar cases can be made of other neuropsychiatric illnesses. For instance, studies of patients with Lewy bodies dementia demonstrated changes in dynamic functional connectivity in the occipito-parieto-frontal and medial occipital networks in addition to the right fronto-parietal circuit, suggesting the importance in characterizing visual and visuomotor dysfunction for the illness (Sourty et al., 2016). In an electroencephalographic study of social anxiety disorder, graphic analysis of a weighted phase lag index demonstrated increased clustering coefficient and decreased characteristic path length in theta-based whole brain functional organization in patients as compared to controls (Xing et al., 2017). Further, the theta-dependent interconnectivity was associated with state anxiety and an increase in information processing efficiency, highlighting a new aspect of attention function, in social anxiety disorder. In a first study of dynamic functional connectivity of Parkinson's disease, the occurrence of sparse within-network connectivity decreased whereas that of the stronger between-network connectivity increased in patients as compared to controls (Kim et al., 2017). The changes reflected a reduction in functional segregation among networks and were correlated with the clinical severity of Parkinson's disease. Again, these findings described vulnerability of network dynamics that have eluded studies focusing solely on the dopaminergic midbrain.

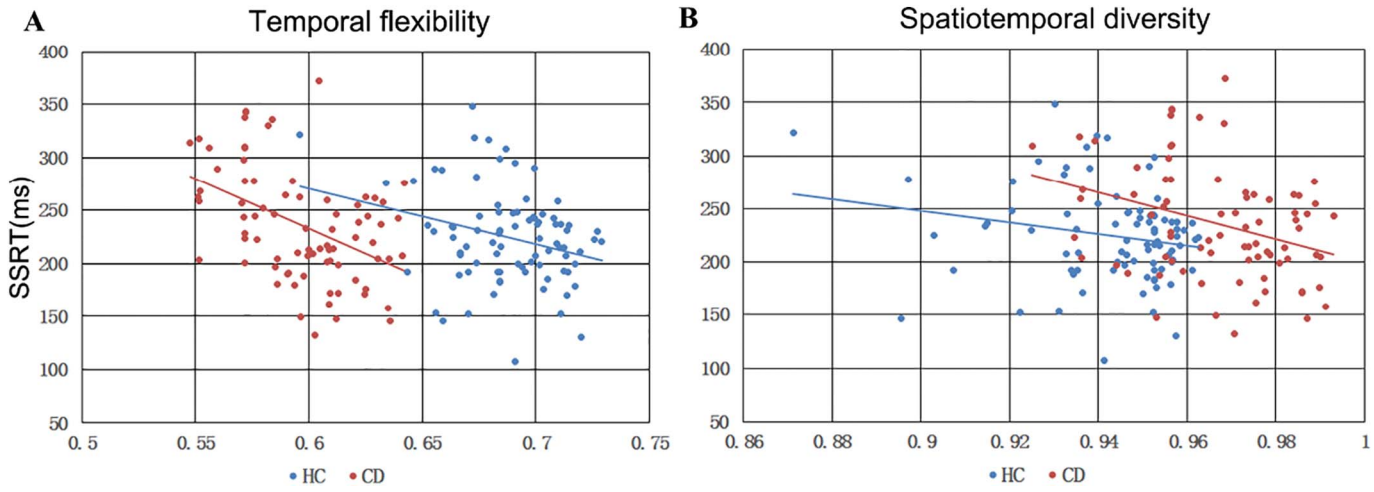

Fig. 3. Linear regression between DMN graph metrics and SSRT. (**A**) temporal flexibility; (**B**) spatiotemporal diversity. Both measures negatively correlated with SSRT in CD.

4.3. Limitations of dynamic connectivity analysis and conclusions

Interpreting temporal variations in functional connectivity (FC) metrics computed from fMRI time series is not necessarily straightforward. Low signal-to-noise ratio, changing levels of non-neural noise (e.g. from hardware instability), as well as variations in the BOLD signal mean and variance over time, all lead to variations in FC metrics (Hutchison et al., 2013). In addition, since functional networks may overlap spatially (i.e., the time series of a single node may have partial correlations with that of multiple networks), the FC between two regions that is attributed to their involvement in one particular network can appear to change if the time series of overlapping networks are not appropriately separated (Xu et al., 2013). Another issue concerns the definition of neural networks. Various atlases defined the networks that are only broadly congruent. It is to be seen whether the current findings would replicate with alternative network definitions. Finally, it remains unclear to what extent dynamic FC is best conceptualized as a multistable state space wherein multiple discrete patterns recur, akin to fixed points of a dynamic system, or whether it simply varies along a continuous state space (Smith et al., 2012).

By demonstrating changes in network connectivity, the current findings may have implications for future research, including those employing electrical and magnetic stimulation and pharmacological interventions (Farr et al., 2014; Kline et al., 2016; Liang et al., 2014). In addition to interrogating how these manipulations may influence regional activity and connectivity, studies can examine graph metrics as neural markers of disease severity and treatment efficacy.

To conclude, analysis of dynamic functional connectivity of fMRI data of the stop signal task characterized changes in network dynamics in relation to impairment in response inhibition in cocaine dependent individuals. The findings highlighted a critical role of the default model network in mediating cognitive control dysfunction in cocaine addiction.

Supplementary data to this article can be found online at https://doi.org/10.1016/j.nicl.2018.03.016.

Acknowledgements

This study was supported by NIH grants DA023248, DA040032, EB022911 as well as research funding provided by Beijing Institute of Technology and NSFC grant 81471743, and by the CT Department of Health and Human Services. We thank Drs. Tienwen Chen and Weidong Cai for discussions on data analysis. The funding agencies had no further roles in study design; in the collection, analysis and interpretation of data; in the writing of the report; or in the decision to submit the paper for publication.

References

Adinoff, B., Gu, H., Merrick, C., McHugh, M., Jeon-Slaughter, H., Lu, H., Yang, Y., Stein, E.A., 2015. Basal hippocampal activity and its functional connectivity predicts cocaine relapse. Biol. Psychiatry 78, 496–504.

Albein-Urios, N., Verdejo-Roman, J., Asensio, S., Soriano-Mas, C., Martinez-Gonzalez, J.M., Verdejo-Garcia, A., 2014. Re-appraisal of negative emotions in cocaine dependence: dysfunctional corticolimbic activation and connectivity. Addict. Biol. 19, 415–426.

Allen, E.A., Damaraju, E., Plis, S.M., Erhardt, E.B., Eichele, T., Calhoun, V.D., 2014. Tracking whole-brain connectivity dynamics in the resting state. Cereb. Cortex 24, 663–676.

Alnaes, D., Kaufmann, T., Richard, G., Duff, E.P., Sneve, M.H., Endestad, T., Nordvik, J.E., Andreassen, O.A., Smith, S.M., Westlye, L.T., 2015. Attentional load modulates large-scale functional brain connectivity beyond the core attention networks. NeuroImage 109, 260–272.

Ashburner, J., Friston, K.J., 1999. Nonlinear spatial normalization using basis functions. Hum. Brain Mapp. 7, 254–266.

Barros-Loscertales, A., Bustamante, J.C., Ventura-Campos, N., Llopis, J.J., Parcet, M.A., Avila, C., 2011. Lower activation in the right frontoparietal network during a counting Stroop task in a cocaine-dependent group. Psychiatry Res. 194, 111–118.

Bassett, D.S., Wymbs, N.F., Porter, M.A., Mucha, P.J., Carlson, J.M., Grafton, S.T., 2011. Dynamic reconfiguration of human brain networks during learning. Proc. Natl. Acad. Sci. U. S. A. 108, 7641–7646.

Bassett, D.S., Yang, M., Wymbs, N.F., Grafton, S.T., 2015. Learning-induced autonomy of sensorimotor systems. Nat. Neurosci. 18, 744–751.

Bednarski, S.R., Zhang, S., Hong, K.I., Sinha, R., Rounsaville, B.J., Li, C.S., 2011. Deficits in default mode network activity preceding error in cocaine dependent individuals. Drug Alcohol Depend. 119, e51–57.

Bednarski, S.R., Erdman, E., Luo, X., Zhang, S., Hu, S., Li, C.S., 2012. Neural processes of an indirect analog of risk taking in young nondependent adult alcohol drinkers-an FMRI study of the stop signal task. Alcohol. Clin. Exp. Res. 36, 768–779.

Berlingeri, M., Losasso, D., Girolo, A., Cozzolino, E., Masullo, T., Scotto, M., Sberna, M., Bottini, G., Paulesu, E., 2017. Resting state brain connectivity patterns before eventual relapse into cocaine abuse. Behav. Brain Res. 327, 121–132.

Braun, U., Schäfer, A., Walter, H., Erk, S., Romanczuk-Seiferth, N., Haddad, L., Schweiger, J.I., Grimm, O., Heinz, A., Tost, H., Meyer-Lindenberg, A., Bassett, D.S., 2015. Dynamic reconfiguration of frontal brain networks during executive cognition in humans. Proc. Natl. Acad. Sci. U. S. A. 112, 11678–11683.

Cai, W., Ryali, S., Chen, T., Li, C.S., Menon, V., 2014. Dissociable roles of right inferior frontal cortex and anterior insula in inhibitory control: evidence from intrinsic and task-related functional parcellation, connectivity, and response profile analyses across multiple datasets. J. Neurosci. 34, 14652–14667.

Cai, W., Chen, T., Ryali, S., Kochalka, J., Li, C.S., Menon, V., 2016. Causal interactions within a frontal-cingulate-parietal network during cognitive control: convergent evidence from a multisite-multitask investigation. Cereb. Cortex 26, 2140–2153.

Cai, W., Chen, T., Ide, J.S., Li, C.R., Menon, V., 2017. Dissociable fronto-operculum-insula control signals for anticipation and detection of inhibitory sensory cue. Cereb. Cortex 27, 4073–4082.

Caldwell, B.M., Harenski, C.L., Harenski, K.A., Fede, S.J., Steele, V.R., Koenigs, M.R., Kiehl, K.A., 2015. Abnormal frontostriatal activity in recently abstinent cocaine users during implicit moral processing. Front. Hum. Neurosci. 9, 565.

Calhoun, V.D., Miller, R., Pearlson, G., Adali, T., 2014. The chronnectome: time-varying connectivity networks as the next frontier in fMRI data discovery. Neuron 84, 262–274.

Chang, C., Glover, G.H., 2010. Time-frequency dynamics of resting-state brain connectivity measured with fMRI. NeuroImage 50, 81–98.

Chen, T., Cai, W., Ryali, S., Supekar, K., Menon, V., 2016. Distinct global brain dynamics and spatiotemporal organization of the salience network. PLoS Biol. 14, e1002469.

Cisler, J.M., Elton, A., Kennedy, A.P., Young, J., Smitherman, S., Andrew James, G., Kilts, C.D., 2013. Altered functional connectivity of the insular cortex across prefrontal networks in cocaine addiction. Psychiatry Res. 213, 39–46.

Cohen, J.R., 2017. The behavioral and cognitive relevance of time-varying, dynamic changes in functional connectivity. NeuroImage. http://dx.doi.org/10.1016/j.neuroimage.2017.09.036. Sep 21. pii: S1053-8119(17)30784-X. [Epub ahead of print].

Contreras-Rodriguez, O., Albein-Urios, N., Perales, J.C., Martinez-Gonzalez, J.M., Vilar-Lopez, R., Fernandez-Serrano, M.J., Lozano-Rojas, O., Verdejo-Garcia, A., 2015. Cocaine-specific neuroplasticity in the ventral striatum network is linked to delay discounting and drug relapse. Addiction 110, 1953–1962.

Crunelle, C.L., Kaag, A.M., van den Munkhof, H.E., Reneman, L., Homberg, J.R., Sabbe, B., van den Brink, W., van Wingen, G., 2015. Dysfunctional amygdala activation and connectivity with the prefrontal cortex in current cocaine users. Hum. Brain Mapp. 36, 4222–4230.

Damaraju, E., Allen, E.A., Belger, A., Ford, J.M., McEwen, S., Mathalon, D.H., Mueller, B.A., Pearlson, G.D., Potkin, S.G., Preda, A., Turner, J.A., Vaidya, J.G., van Erp, T.G., Calhoun, V.D., 2014. Dynamic functional connectivity analysis reveals transient states of dysconnectivity in schizophrenia. Neurol. Clin. 5, 298–308.

Duann, J.R., Ide, J.S., Luo, X., Li, C.S., 2009. Functional connectivity delineates distinct roles of the inferior frontal cortex and presupplementary motor area in stop signal inhibition. J. Neurosci. 29, 10171–10179.

Farr, O.M., Zhang, S., Hu, S., Matuskey, D., Abdelghany, O., Malison, R.T., Li, C.S., 2014. The effects of methylphenidate on resting-state striatal, thalamic and global functional connectivity in healthy adults. Int. J. Neuropsychopharmacol. 17, 1177–1191.

Fornito, A., Harrison, B.J., Zalesky, A., Simons, J.S., 2012. Competitive and cooperative dynamics of large-scale brain functional networks supporting recollection. Proc. Natl. Acad. Sci. U. S. A. 109, 12788–12793.

Friston, K.J., Holmes, A.P., Poline, J.B., Grasby, P.J., Williams, S.C., Frackowiak, R.S., Turner, R., 1995. Analysis of fMRI time-series revisited. NeuroImage 2, 45–53.

Geng, X., Hu, Y., Gu, H., Salmeron, B.J., Adinoff, B., Stein, E.A., Yang, Y., 2017. Salience and default mode network dysregulation in chronic cocaine users predict treatment outcome. Brain 140 (5), 1513–1524.

Hu, S., Tseng, Y.C., Winkler, A.D., Li, C.S., 2014. Neural bases of individual variation in decision time. Hum. Brain Mapp. 35, 2531–2542.

Hu, S., Ide, J.S., Zhang, S., Li, C.S., 2015a. Anticipating conflict: neural correlates of a Bayesian belief and its motor consequence. NeuroImage 119, 286–295.

Hu, S., Ide, J.S., Zhang, S., Sinha, R., Li, C.S., 2015b. Conflict anticipation in alcohol dependence - a model-based fMRI study of stop signal task. Neurol. Clin. 8, 39–50.

Hu, Y., Salmeron, B.J., Gu, H., Stein, E.A., Yang, Y., 2015c. Impaired functional connectivity within and between frontostriatal circuits and its association with compulsive drug use and trait impulsivity in cocaine addiction. JAMA Psychiat. 72, 584–592.

Hu, S., Ide, J.S., Zhang, S., Li, C.R., 2016. The right superior frontal gyrus and individual variation in proactive control of impulsive response. J. Neurosci. 36, 12688–12696.

Hutchison, R.M., Womelsdorf, T., Allen, E.A., Bandettini, P.A., Calhoun, V.D., Corbetta, M., Penna, S.D., Duyn, J.H., Glover, G.H., Gonzalez-Castillo, J., Handwerker, D.A., Keilholz, S., Kiviniemi, V., Leopold, D.A., de Pasquale, F., Sporns, O., Walter, M., Chang, C., 2013. Dynamic functional connectivity: promise, issues, and interpretations. NeuroImage 80.

Ide, J.S., Shenoy, P., Yu, A.J., Li, C.S., 2013. Bayesian prediction and evaluation in the

anterior cingulate cortex. J. Neurosci. 33, 2039–2047.
Ide, J.S., Hu, S., Zhang, S., Yu, A.J., Li, C.S., 2015. Impaired Bayesian learning for cognitive control in cocaine dependence. Drug Alcohol Depend. 151, 220–227.
Ide, J.S., Hu, S., Zhang, S., Mujica-Parodi, L.R., Li, C.S., 2016. Power spectrum scale invariance as a neural marker of cocaine misuse and altered cognitive control. Neurol. Clin. 11, 349–356.
Kaiser, R.H., Whitfield-Gabrieli, S., Dillon, D.G., Goer, F., Beltzer, M., Minkel, J., Smoski, M., Dichter, G., Pizzagalli, D.A., 2016. Dynamic resting-state functional connectivity in major depression. Neuropsychopharmacology 41, 1822–1830.
Kang, J., Wang, L., Yan, C., Wang, J., Liang, X., He, Y., 2011. Characterizing dynamic functional connectivity in the resting brain using variable parameter regression and Kalman filtering approaches. NeuroImage 56, 1222–1234.
Kim, J., Criaud, M., Cho, S.S., Diez-Cirarda, M., Mihaescu, A., Coakeley, S., Ghadery, C., Valli, M., Jacobs, M.F., Houle, S., Strafella, A.P., 2017. Abnormal intrinsic brain functional network dynamics in Parkinson's disease. Brain 140, 2955–2967.
Kline, R.L., Zhang, S., Farr, O.M., Hu, S., Zaborszky, L., Samanez-Larkin, G.R., Li, C.S., 2016. The effects of methylphenidate on resting-state functional connectivity of the basal nucleus of Meynert, locus coeruleus, and ventral tegmental area in healthy adults. Front. Hum. Neurosci. 10, 149.
Konova, A.B., Moeller, S.J., Tomasi, D., Goldstein, R.Z., 2015. Effects of chronic and acute stimulants on brain functional connectivity hubs. Brain Res. 1628, 147–156.
de Lacy, N., Doherty, D., King, B.H., Rachakonda, S., Calhoun, V.D., 2017. Disruption to control network function correlates with altered dynamic connectivity in the wider autism spectrum. Neurol. Clin. 15, 513–524.
Lench, D.H., DeVries, W., Hanlon, C.A., 2017. The effect of task difficulty on motor performance and frontal-striatal connectivity in cocaine users. Drug Alcohol Depend. 173, 178–184.
Li, C.S., Yan, P., Bergquist, K.L., Sinha, R., 2007. Greater activation of the “default” brain regions predicts stop signal errors. NeuroImage 38, 640–648.
Li, C.S., Huang, C., Yan, P., Bhagwagar, Z., Milivojevic, V., Sinha, R., 2008. Neural correlates of impulse control during stop signal inhibition in cocaine-dependent men. Neuropsychopharmacology 33, 1798–1806.
Liang, W.K., Lo, M.T., Yang, A.C., Peng, C.K., Cheng, S.K., Tseng, P., Juan, C.H., 2014. Revealing the brain's adaptability and the transcranial direct current stimulation facilitating effect in inhibitory control by multiscale entropy. NeuroImage 90, 218–234.
Liang, X., He, Y., Salmeron, B.J., Gu, H., Stein, E.A., Yang, Y., 2015. Interactions between the salience and default-mode networks are disrupted in cocaine addiction. J. Neurosci. 35, 8081–8090.
Ma, L., Steinberg, J.L., Hasan, K.M., Narayana, P.A., Kramer, L.A., Moeller, F.G., 2014. Stochastic dynamic causal modeling of working memory connections in cocaine dependence. Hum. Brain Mapp. 35, 760–778.
Ma, L., Steinberg, J.L., Cunningham, K.A., Lane, S.D., Bjork, J.M., Neelakantan, H., Price, A.E., Narayana, P.A., Kosten, T.R., Bechara, A., Moeller, F.G., 2015. Inhibitory behavioral control: a stochastic dynamic causal modeling study comparing cocaine dependent subjects and controls. Neurol. Clin. 7, 837–847.
Mattar, M.G., Cole, M.W., Thompson-Schill, S.L., Bassett, D.S., 2015. A functional cartography of cognitive systems. PLoS Comput. Biol. 11.
Matuskey, D., Luo, X., Zhang, S., Morgan, P.T., Abdelghany, O., Malison, R.T., Li, C.S., 2013. Methylphenidate remediates error-preceding activation of the default mode brain regions in cocaine-addicted individuals. Psychiatry Res. 214, 116–121.
McHugh, M.J., Demers, C.H., Salmeron, B.J., Devous Sr., M.D., Stein, E.A., Adinoff, B., 2014. Cortico-amygdala coupling as a marker of early relapse risk in cocaine-addicted individuals. Front. Psych. 5, 16.
McHugh, M.J., Gu, H., Yang, Y., Adinoff, B., Stein, E.A., 2017. Executive control network connectivity strength protects against relapse to cocaine use. Addict. Biol. 22 (6), 1790–1801.
Menon, V., Uddin, L.Q., 2010. Saliency, switching, attention and control: a network model of insula function. Brain Struct. Funct. 214, 655–667.
Morgan, V.L., Abou-Khalil, B., Rogers, B.P., 2015. Evolution of functional connectivity of brain networks and their dynamic interaction in temporal lobe epilepsy. Brain Connect. 5, 35–44.
Mucha, P.J., Richardson, T., Macon, K., Porter, M.A., Onnela, J.P., 2010. Community structure in time-dependent, multiscale, and multiplex networks. Science 328, 876–878.
Newman, M.E., 2004. Fast algorithm for detecting community structure in networks. Phys. Rev. E Stat. Nonlinear Soft Matter Phys. 69, 066133.
Nomi, J.S., Farrant, K., Damaraju, E., Rachakonda, S., Calhoun, V.D., Uddin, L.Q., 2016. Dynamic functional network connectivity reveals unique and overlapping profiles of insula subdivisions. Hum. Brain Mapp. 37, 1770–1787.
Power, J.D., Cohen, A.L., Nelson, S.M., Wig, G.S., Barnes, K.A., Church, J.A., Vogel, A.C., Laumann, T.O., Miezin, F.M., Schlaggar, B.L., Petersen, S.E., 2011. Functional network organization of the human brain. Neuron 72, 665–678.
Power, J.D., Schlaggar, B.L., Lessov-Schlaggar, C.N., Petersen, S.E., 2013. Evidence for hubs in human functional brain networks. Neuron 79, 798–813.
Ray, S., Gohel, S., Biswal, B.B., 2015a. Altered functional connectivity strength in abstinent chronic cocaine smokers compared to healthy controls. Brain Connect. 5, 476–486.
Ray, S., Haney, M., Hanson, C., Biswal, B., Hanson, S.J., 2015b. Modeling causal relationship between brain regions within the drug-cue processing network in chronic cocaine smokers. Neuropsychopharmacology 40, 2960–2968.
Ray, S., Di, X., Biswal, B.B., 2016. Effective connectivity within the mesocorticolimbic system during resting-state in cocaine users. Front. Hum. Neurosci. 10, 563.
Rosell-Negre, P., Bustamante, J.C., Fuentes-Claramonte, P., Costumero, V., Llopis-Llacer, J.J., Barros-Loscertales, A., 2016. Reward contingencies improve goal-directed behavior by enhancing posterior brain attentional regions and increasing corticostriatal connectivity in cocaine addicts. PLoS One 11, e0167400.
Rubinov, M., Sporns, O., 2010. Complex network measures of brain connectivity: uses and interpretations. NeuroImage 52, 1059–1069.
Sakoğlu, Ü., Pearlson, G.D., Kiehl, K.A., Wang, Y.M., Michael, A.M., Calhoun, V.D., 2010. A method for evaluating dynamic functional network connectivity and task-modulation: application to schizophrenia. MAGMA 23, 351–366.
Smith, S.M., Miller, K.L., Moeller, S., Xu, J., Auerbach, E.J., Woolrich, M.W., Beckmann, C.F., Jenkinson, M., Andersson, J., Glasser, M.F., Van Essen, D.C., Feinberg, D.A., Yacoub, E.S., Ugurbil, K., 2012. Temporally-independent functional modes of spontaneous brain activity. Proc. Natl. Acad. Sci. U. S. A. 109, 3131–3136.
Sourty, M., Thoraval, L., Roquet, D., Armspach, J.P., Foucher, J., Blanc, F., 2016. Identifying dynamic functional connectivity changes in dementia with Lewy bodies based on product hidden Markov models. Front. Comput. Neurosci. 10, 60.
Thompson, G.J., Magnuson, M.E., Merritt, M.D., Schwarb, H., Pan, W.J., McKinley, A., Tripp, L.D., Schumacher, E.H., Keilholz, S.D., 2013. Short-time windows of correlation between large-scale functional brain networks predict vigilance intraindividually and interindividually. Hum. Brain Mapp. 34, 3280–3298.
Winkler, A.D., Hu, S., Li, C.S., 2013. The influence of risky and conservative mental sets on cerebral activations of cognitive control. Int. J. Psychophysiol. 87, 254–261.
Wisner, K.M., Patzelt, E.H., Lim, K.O., MacDonald 3rd, A.W., 2013. An intrinsic connectivity network approach to insula-derived dysfunctions among cocaine users. Am. J. Drug Alcohol Abuse 39, 403–413.
Xing, M., Tadayonnejad, R., MacNamara, A., Ajilore, O., DiGangi, J., Phan, K.L., Leow, A., Klumpp, H., 2017. Resting-state theta band connectivity and graph analysis in generalized social anxiety disorder. Neurol. Clin. 13, 24–32.
Xu, J., Zhang, S., Calhoun, V.D., Monterosso, J., Li, C.S., Worhunsky, P.D., Stevens, M., Pearlson, G.D., Potenza, M.N., 2013. Task-related concurrent but opposite modulations of overlapping functional networks as revealed by spatial ICA. NeuroImage 79, 62–71.
Yaesoubi, M., Miller, R.L., Bustillo, J., Lim, K.O., Vaidya, J., Calhoun, V.D., 2017. A joint time-frequency analysis of resting-state functional connectivity reveals novel patterns of connectivity shared between or unique to schizophrenia patients and healthy controls. Neurol. Clin. 15, 761–768.
Zalesky, A., Fornito, A., Cocchi, L., Gollo, L.L., Breakspear, M., 2014. Time-resolved resting-state brain networks. Proc. Natl. Acad. Sci. U. S. A. 111, 10341–10346.
Zhang, S., Li, C.S., 2010. A neural measure of behavioral engagement: task-residual low-frequency blood oxygenation level-dependent activity in the precuneus. NeuroImage 49, 1911–1918.
Zhang, S., Li, C.S., 2012. Task-related, low-frequency task-residual, and resting state activity in the default mode network brain regions. Front. Psychol. 3, 172.
Zhang, S., Hu, S., Bednarski, S.R., Erdman, E., Li, C.S., 2014. Error-related functional connectivity of the thalamus in cocaine dependence. Neurol. Clin. 4, 585–592.
Zhang, S., Hu, S., Sinha, R., Potenza, M.N., Malison, R.T., Li, C.S., 2016. Cocaine dependence and thalamic functional connectivity: a multivariate pattern analysis. Neurol. Clin. 12, 348–358.